Geo-Mar Lett
DOI 10.1007/s00367-016-0435-9

ORIGINAL

Drones as tools for monitoring beach topography changes in the Ligurian Sea (NW Mediterranean)

Elisa Casella[1,2] · **Alessio Rovere**[1,3,4] · **Andrea Pedroncini**[5] · **Colin P. Stark**[4] · **Marco Casella**[6] · **Marco Ferrari**[7] · **Marco Firpo**[7]

Received: 2 September 2015 / Accepted: 13 January 2016

Abstract The aim of this study was to evaluate topographic changes along a stretch of coastline in the Municipality of Borghetto Santo Spirito (Region of Liguria, Italy, northwestern Mediterranean) by means of a remotely piloted aircraft system coupled with structure from motion and multi-view stereo techniques. This sector was surveyed three times over 5 months in the fall–winter of 2013–2014 (1 November 2013, 4 December 2013, 17 March 2014) to obtain digital elevation models and orthophotos of the beach. Changes in beach topography associated with storm action and human activities were assessed in terms of gain/loss of sediments and shifting of the wet–dry boundary defining the shoreline. Between the first and second surveys, the study area was hit by two storms (10–11 November 2013 and 21–22 November 2013) with waves approaching from the E–NNE, causing a shoreline retreat which, in some sectors, reached 7 m. Between the second and third surveys, by contrast, four storms (25–27 December 2013, 5–6 January 2014, 17–18 January 2014 and 6–10 February 2014) with waves propagating from the SE produced a general advancement of the shoreline (up to ~5 m) by deposition of sediments along some parts of the beach. The data also reflect changes in beach topography due to human activity during the 2013 fall season, when private beach managers quarried ~178 m^3 of sediments on the emerged beach near the shoreline to accumulate them landwards. The results show that drones can be used for regular beach monitoring activities, and that they can provide new insights into the processes related to natural and/or human-related topographic beach changes.

✉ Elisa Casella
elisacasellaphd@gmail.com

1 ZMT, Leibniz Center for Tropical Marine Ecology, Bremen, Germany

2 SEAMap srl, Environmental Consulting, Borghetto Santo Spirito, SV, Italy

3 MARUM, University of Bremen, Bremen, Germany

4 Lamont-Doherty Earth Observatory, Columbia University, Palisades, NY, USA

5 DHI-Italia, Genova, Italy

6 Freelancer and Professional UAV Pilot, Tovo S. Giacomo, SV, Italy

7 DISTAV, University of Genoa, Genova, Italy

Introduction

Coastal erosion is one of the main natural processes defining the evolution of a shoreline through time. Along beaches, erosion removes sediment from the coastal system and transports it offshore through the action of waves and currents. In general, coastal erosion is considered a problem in need of management when it occurs in densely populated areas. On a global scale, the population density within 100 km of the coastline is nearly three times higher than the average density (Small and Nicholls 2003), and 10% of the human population today lives less than 10 m above sea level (McGranahan et al. 2007). Already in the late 1980s, the benchmark study of Bird (1987) identified that 70% of the world's beaches are affected by erosion problems.

Coastal management and decision-making are often based on studies investigating the rates and modes of coastal changes derived from various beach monitoring techniques, either direct (i.e. GPS surveys or topographic transects) or indirect (e.g. lidar or aerial photography). Thus, techniques for beach monitoring are based on either in situ observations or remotely sensed data. Among the former, the most popular are high-accuracy GPS surveys (Morton et al. 1993; Harley et al. 2010), total stations or terrestrial laser scanners (Saye et al. 2005; Theuerkauf and Rodriguez 2012; Lee et al. 2013). These techniques are relatively inexpensive and have a good accuracy (2–6 cm vertical; Lee et al. 2013) but require large

Published online: 26 January 2016

efforts to map wide areas, and also do not provide orthophotos useful in detecting specific elements of the terrain. Common techniques to monitor larger areas over shorter time intervals are those employing remotely sensed data, such as aerial photographs and webcam images (Hapke and Richmond 2000; Alexander and Holman 2004; Kroon et al. 2007; Taborda and Silva 2012; Turki et al. 2013), satellite images taken at different times (Blodget et al. 1991), and airborne lidar mapping (Stockdon et al. 2002; Young and Ashford 2006). Their main limitations are their relatively high costs and the commonly insufficient availability of images spanning periods of interest. Remote-sensing instruments mounted on satellites, spacecrafts or manned aircraft provide useful information to assess coastal processes at global to regional scales (Wulder et al. 2004) but some processes need to be studied at a more local scale, often requiring multi-temporal observations spanning short time intervals which cannot be delivered by satellites or manned flights (Anderson and Gaston 2013).

Recently, new survey techniques based on remotely piloted aircraft systems (RPAS, also called unmanned aerial vehicles, UAVs, or drones: in the text, these terms are used as synonyms) have begun to be employed in geomorphological and ecological studies (Everaerts 2008; Colomina and Molina 2014; Anderson and Gaston 2013; Floreano and Wood 2015), and are becoming common survey tools in the geosciences. The standard geomorphological application of RPAS consists in mounting a camera on a rotor-wing or fixed-wing remotely controlled or programmed aircraft and taking almost-nadir pictures of the ground which are then analyzed with structure from motion (SfM) and multi-view stereo (MVS) reconstruction algorithms to obtain digital elevation models (DEMs) and orthophotos of the terrain. SfM and MVS methods represent a major advancement in the field of photogrammetry for geoscience applications (James and Robson 2012; Westoby et al. 2012). James and Robson (2012) reported that these methods produce results similar to those of more traditional topographic techniques (laser scanner), while reducing data collection time by 80%. In the field of computer science, these methods have advanced together with the development of drone platforms which are now closing the gaps in small-scale remote sensing (Berni et al. 2009; Watts et al. 2012) because they enable the acquisition of high-resolution data at low altitudes and, moreover, their relatively low cost facilitates repeated surveys over short time intervals.

At present, studies are going beyond the simple assessment of the accuracy of orthophotos and DEMs which can be obtained with RPAS coupled with SfM and MVS techniques, RPAS being used to obtain data addressing specific environmental or geological problems (Niethammer et al. 2012; Casella et al. 2014; Pérez-Alberti and Trenhaile 2015; Eltner et al. 2015; Woodget et al. 2015). The coastal zone is an ideal ground for the application of multi-temporal RPAS surveys, as the evolution of these environments is often fast, requiring efficient, low-cost and sufficiently accurate monitoring techniques.

The aim of this paper is to assess topographic changes (gain/loss of sediment, and shoreline variations) of a beach in the Municipality of Borghetto Santo Spirito (Region of Liguria, Italy) by means of a RPAS coupled with SfM, MVS and GIS techniques. Topographic changes are evaluated in terms of storm events and human activities. This work expands on an earlier study by Casella et al. (2014) which focussed on coastal flooding at another location within the same general study area.

Study area and background

Coastal setting

The study area is located in Liguria, an administrative region of Italy in the NW Mediterranean (Fig. 1a). The NW Mediterranean is one of the most cyclogenetic areas of the Mediterranean basin (Trigo et al. 2002). As a result, the Region of Liguria often experiences severe storms (Parodi et al. 2012; Rebora et al. 2013; Fiori et al. 2014) causing major damages to the coastal zone and endangering the human population (Orlandi et al. 2008; Pasi et al. 2011). These events are more frequent during the winter and fall seasons (Littmann 2000).

The Ligurian coastline is mainly exposed to winds blowing from the southern quadrants. As a consequence, the dominant wave direction is from the SW (220–240°N). From this direction the fetch is about 800 km and the significant offshore wave height is >3 m. Waves from the SE (130–150°N) have a fetch of 200 km and significant offshore wave heights of >2 m, whereas waves from the south (180°N) are much less frequent and have lower significant wave heights (Vacchi et al. 2010, 2014). Waves propagating from the SW are thus the most intense and frequent, followed by waves from the SE (Corsini et al. 2006; Ferrari et al. 2014). The wave characteristics of the Ligurian Sea reflect the strong seasonality of the weather regime (Sartini et al. 2014).

In the present study, the sea state during the fall–winter seasons of 2013–2014 was recorded and modelled (see modelled area in Fig. 1a). Between 1 November 2013 and 17 March 2014, six events with a significant wave high between 2 and 5 m were registered by an offshore buoy at Capo Mele (10–11 November 2013, 21–22 November 2013, 25–27 December 2013, 5–6 January 2014, 17–18 January 2014 and 6–10 February 2014).

Due to marked coastal erosion problems in the region, several research initiatives have been directed towards both understanding the coastal dynamics (e.g. Brignone et al. 2012) and monitoring coastal evolution with various techniques (e.g. Vacchi et al. 2012; Casella et al. 2014). Recently, the Liguria

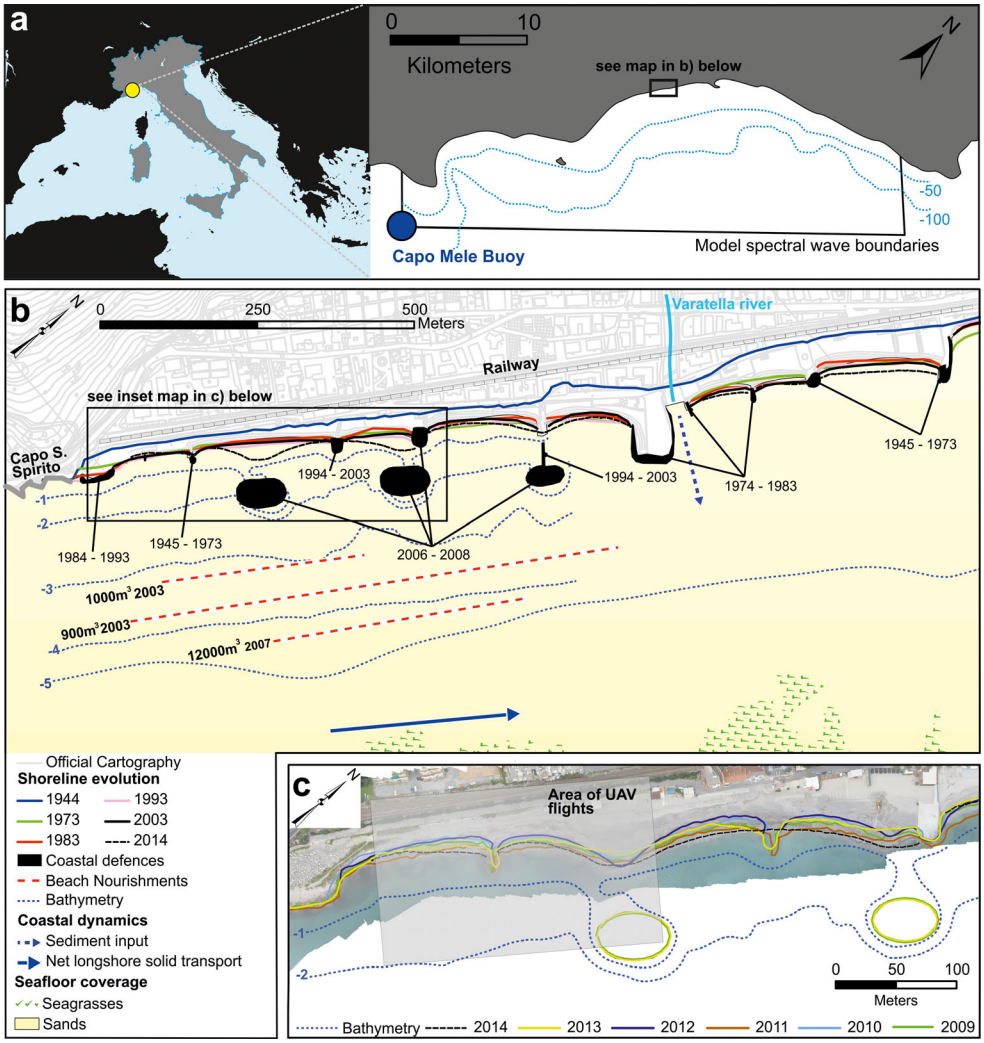

Fig. 1 **a** Location of study area in the north-western Mediterranean Sea, including the area where the spectral wave model described in the paper has been implemented. **b** The shoreline and nearshore area of Borghetto Santo Spirito, showing the main geological and biological bottom features (Rovere et al. 2014), the shoreline traced as wet–dry line on orthophotos (1944–2003, data from Regione Liguria), the shoreline surveyed with DGPS in June 2014 (this study, see Fig. 5), and coastal defences and their year of construction (data from Regione Liguria). *Dashed blue arrow* Main sedimentary input from the Varatella River, *solid blue arrow* main littoral drift (Rovere et al. 2014), *dashed red lines* beach nourishment sites where sediment has been dumped onshore (labels indicate the year and quantity of sediment used; data from Regione Liguria). **c** Detail of **b**, with area of RPAS flights. The shoreline and bathymetric data have been provided by the Municipality of Borghetto S.S. The shoreline represents the wet–dry line surveyed in different years with DGPS. All data are either original or have been derived by public archives (www.ambienteinliguria.it)

regional authority has made available vector files of the shoreline (wet–dry line) extracted from orthophotos made in 1944, 1973, 1983 and 2003 (Fig. 1b). The first flight was carried out by the UK Royal Air Force during WWII. Later flights were aimed at documenting shoreline changes rooted in the economic boom of the 1960s and 1970s, accompanied by exponential increases in both the local population and tourism (Fierro et al. 2010).

Coastal evolution

The evolution of the coastal area of Borghetto Santo Spirito is representative of many northern Mediterranean coastal sites. Borghetto was a small village at the end of 17th Century, when a railroad was constructed to connect the main cities of Genoa (Italy, to the east) and Nice (France, to the west). Construction materials were quarried from a local watercourse, the Varatella River, causing a reduction of sediment input in the beach budget. This led to the erosion of the coastline (Fierro et al. 2010). Since those times, the coastline has been affected by engineering works (e.g. groynes, parallel defences) primarily aimed at protecting the railway from storm waves. In 1944, the shoreline was located close to the railway (Fig. 1b). From the 1960s to today, the shoreline has been object of several interventions, especially beach nourishment and coastal engineering to promote the creation and maintenance of beaches which began to be exploited for

touristic purposes (Fig. 1b; Fierro et al. 2010). The most recent engineering works (2006–2008) are three artificial islands located near the western part of the town (Fig. 1b, c), resulting from two major beach nourishments in 2003 and 2007 (Fig. 1b) when a total amount of 13,900 m^3 of sediment were discharged in the area. This part of the coast is most affected by erosion problems, as all sediment inputs are blocked by a rocky promontory (Capo Santo Spirito) to the west and by a major groyne to the east, which blocks the input of sediments from the Varatella River.

As the objective of repeated beach interventions was to mitigate coastal erosion, the westernmost part of the town (Fig. 1c) was subject of several beach monitoring campaigns ordered by the municipal authority. These consisted mostly of differential GPS (DGPS) surveys of the wet–dry line and bathymetric surveys. The results of those surveys (Fig. 1c) indicated that, following the interventions in this area, the shoreline had advanced and now fluctuates yearly around a new equilibrium. Today, the sediments of the beaches of Borghetto are predominantly composed of coarse to very coarse sand (90–95%; Vacchi et al. 2010).

Ever since the beaches began to be exploited for tourism in the 1960s, there has been the need to both monitor and quantify beach erosion which occurs mainly during winter storms. To counteract the loss of sand due to storm action, large volumes of sediment are moved from the emerged beach near the shoreline to the landward part of the beach with excavators at the end of the touristic season (October), only to be returned towards the shoreline in spring before the beginning of the new tourist season. Removing, nourishing or moving sediments on the beach is considered by law analogous to normal beach nourishment (regional laws 13/1999, 6/2001, 3/2007 and 5/2011, which obey national and EU framework directives). The regional laws state that, if more than 10 m^3 of sediment per linear meter are removed, added or moved on the shore, the authority in charge is required to perform an environmental evaluation including description of the site, source and quantity of sediment involved, and consideration of potentially threatened habitats or species. One of the main difficulties for regional environmental agencies is to control the 10 m^3 sediment threshold. If this threshold is surpassed and no environmental evaluation is done, then the law enforces appropriate penalties.

Materials and methods

RPAS, photogrammetry and GIS tools

A RPAS (Mikrokopter Okto XL) equipped with a Canon G11 camera served to obtain aerial photographs with a 3,648×2,736 pixel resolution. The camera has an ultra high-resolution 10.0-megapixel CCD sensor and a 28 mm wide-angle lens (35 mm film equivalent). The maximum takeoff weight of the RPAS was 1.8 kg. Flights were programmed using the Mikrokopter OSD tools software to cover the entire area shown in Fig. 1c at 70 m altitude, speed of 1 m/s and with one photograph taken automatically every 2 s. The flights were controlled by a pilot and an observer. The pilot had the duty to perform take-off and landing operations, and interrupt the GPS-guided flight in case of unexpected behaviour of the RPAS. The observer had the duty to follow the flight from the ground station and communicate changes from the predefined path to the pilot. An overview of national regulations for RPAS deployment is contained in Colomina and Molina (2014). For a more detailed description of the system used in this study, the reader is referred to Casella et al. (2014).

Agisoft Photoscan (http://www.agisoft.ru) software served to generate DEMs and orthorectified images from near-nadir photos acquired during the flights. In a first step, the software aligns the photographs using an SfM algorithm (Ullman 1979) which identifies image feature points and subsequently monitors the movement of those points throughout the image dataset. Estimation of the camera position is one of the main components in SfM (Hartley and Zisserman 2003; Szeliski 2010). Outputs of this first step are (1) a three-dimensional point cloud representing the geometry of the study area; (2) relative camera positions at the moment of image acquisition; (3) internal calibration parameters (focal length, principal point location, three radial and two tangential distortion coefficients). Because these first processing steps estimate the calibration parameters, there is no real need to apply calibrated cameras and optics during the image acquisition stage (Verhoeven 2011).

The second step builds a dense point cloud. In coastal zone surveys, most images partially cover the sea, which must be excluded from the beach topography. This was done by means of the Photoscan mask function.

In a third step, the algorithms operate on the pixel values to build the majority of geometric details. All pixels are utilized in the MVS reconstruction algorithm (Scharstein and Szeliski 2002; Seitz et al. 2006). The software applies an algorithm based on an advanced computer vision solution which enables the creation of high-quality three-dimensional content from a series of overlapping aerial images (Verhoeven 2011).

In a fourth step, the mesh is textured with the photographs. In order to georeference and evaluate the DEMs and orthophotos produced with Agisoft Photoscan, ground control points (GCPs) and additional control points (CPs) were collected using a GPS system (Trimble ProXRT). For each GPS point, 10 minutes of static data were collected (1 point per second), and post-processed with Trimble Pathfinder Office software using the 1-second data of the GNSS base station 'Istituto G. Falcone' (http://www.gnssliguria.it/postprocessing.html) located 1.5 km from the study area. The final accuracy of the GPS data is better than ±5 cm (XYZ). All the elevations were referred to the EGM 2008 global geoid model.

As targets for the GCPs, fixed structures on the ground such as the centre of sewer covers, mosaics representing the edges of structures, or the centres of boulders forming the

groynes were used (see Figs. 2 and 3). The collected GCPs were subsequently imported in Photoscan and used to georeference the results of the photogrammetric workflow. Table 1 shows the Photoscan workflow and parameters of this study. At the end of the workflow, the orthophotos and DEMs were exported from Photoscan and imported into a GIS software (ArcGis10.2). After the accuracy check described below, differences between the co-registered DEMs were calculated using the ArcGis Raster Calculator toolbox.

Control points (CPs) were collected along continuous GPS transects on invariant surfaces (e.g. concrete structures or walking areas not subject to change during the survey period). The root mean square error (RMSE) between the CPs and the values of the DEM was calculated for each location:

$$RMSE = \sqrt{\frac{\sum_{i=1}^{n} (\mathrm{CP}_i - \mathrm{D}_i)^2}{n}} \quad (1)$$

where CP is the elevation of the control point measured with post-processed GPS data, D the elevation of the DEM at the same point and n the total number of CPs.

During calm weather on 10 June 2014, the same GPS setup used to collect data on CPs and GCPs served to pinpoint the wet–dry line boundary by walking along it. In order to compare the DEMs with the shoreline surveyed with DGPS, the wet–dry line was also traced on the orthophotos. The wet–dry line is the boundary between wet and dry sand. Due to the calm sea conditions during the surveys, the low tidal ranges and the high inclination of the beach profiles, this coincided roughly with mean sea level at the time of the measurements.

In order to place an error constraint on the wet–dry line, the average inclination of the nearshore area was measured in the field, in this case amounting to 9.4°. The tidal range recorded by the nearby gauge of Genova was 0.35 m. Using these two values, the map error of the shorelines obtained from the aerial photos was estimated to be ±1.05 m.

During the surveys, the weather was mainly cloudy with winds less than 20 km/h. Cloudy skies are particularly favourable for SfM-MVS reconstructions because of the absence of shadows. The geomagnetic field, which can interfere with the communications system of the drone platform, was quiet (daily checks available at http://www.n3kl.org/sun/noaa.html).

Wave data and model

Significant wave height, mean wave direction and peak period were downloaded from the Capo Mele buoy, which is part of the Liguria region buoy network (http://servizi-meteoliguria.arpal.gov.it/ boacapomele.html) managed by the regional environmental protection agency (Agenzia Regionale per la Protezione dell'Ambiente Ligure, ARPAL). Since the buoy is located about 20 km south of the study area (43°55′18″N, 8°10′50″E, Fig. 1a) where the complex coastal geomorphology can significantly affect wave propagation, the spectral wave model developed by DHI (https://www.dhigroup.com/), MIKE 21, was implemented to obtain information on waves affecting the study area.

MIKE 21 SW is based on unstructured meshes accommodating different spatial resolution in the same domain, and simulating wave growth by action of wind, nonlinear wave–wave interaction, dissipation due to white-capping, dissipation due to bottom friction, dissipation due to depth-induced wave breaking, refraction and shoaling due to depth variations and wave–current interaction. A directional decoupled parametric formulation suitable for coastal applications was used for wave modelling, based on parameterisation of the wave action conservation equation (Holthuijsen et al. 1989). For full description, see the 'Scientific documentation' of the DHI software (DHI 2012).

In the present study, the simulated area covers about 150 km^2 of the nearshore zone in the north-western Mediterranean (Fig. 1a). The coastline was extracted from the databases available in the Italian Ministry of Environment cartographic portal (www.pcn.mianmbiente.it). Bathymetric data were obtained from the Istituto Idrografico della Marina (Italian National Hydrographic Institute) and, near the coast, from multibeam data by Regione Liguria (Rovere et al. 2014 and Casella et al. 2014). The spatial resolution of the model spans from 500 m offshore to 100 m nearshore. The southeast corner of the domain is located at 43°55′18″N, 8°10′50″E (cf. Capo Mele wave buoy, Fig. 1a).

Results

RPAS flights and DEM accuracy

Each of the three RPAS flights covering the study area (~0.01 km^2) at different times resulted in a total of ~130 photographs shot at ~90° angle. Excluding photos not catching the study area (e.g. before/during takeoff) and blurred photos, 65–70 photos of each flight were available as input to the software workflow. The time to collect a single set of photos was 8 minutes (using one battery for each flight). The survey was repeated on 1 November 2013, 4 December 2013 and 17 March 2014 using the same flight parameters. After comparing the elevation of CPs and DEMs at 254 points, the vertical accuracy of the DEMs was determined to be 0.15–0.16 m (RMSE, Fig. 2).

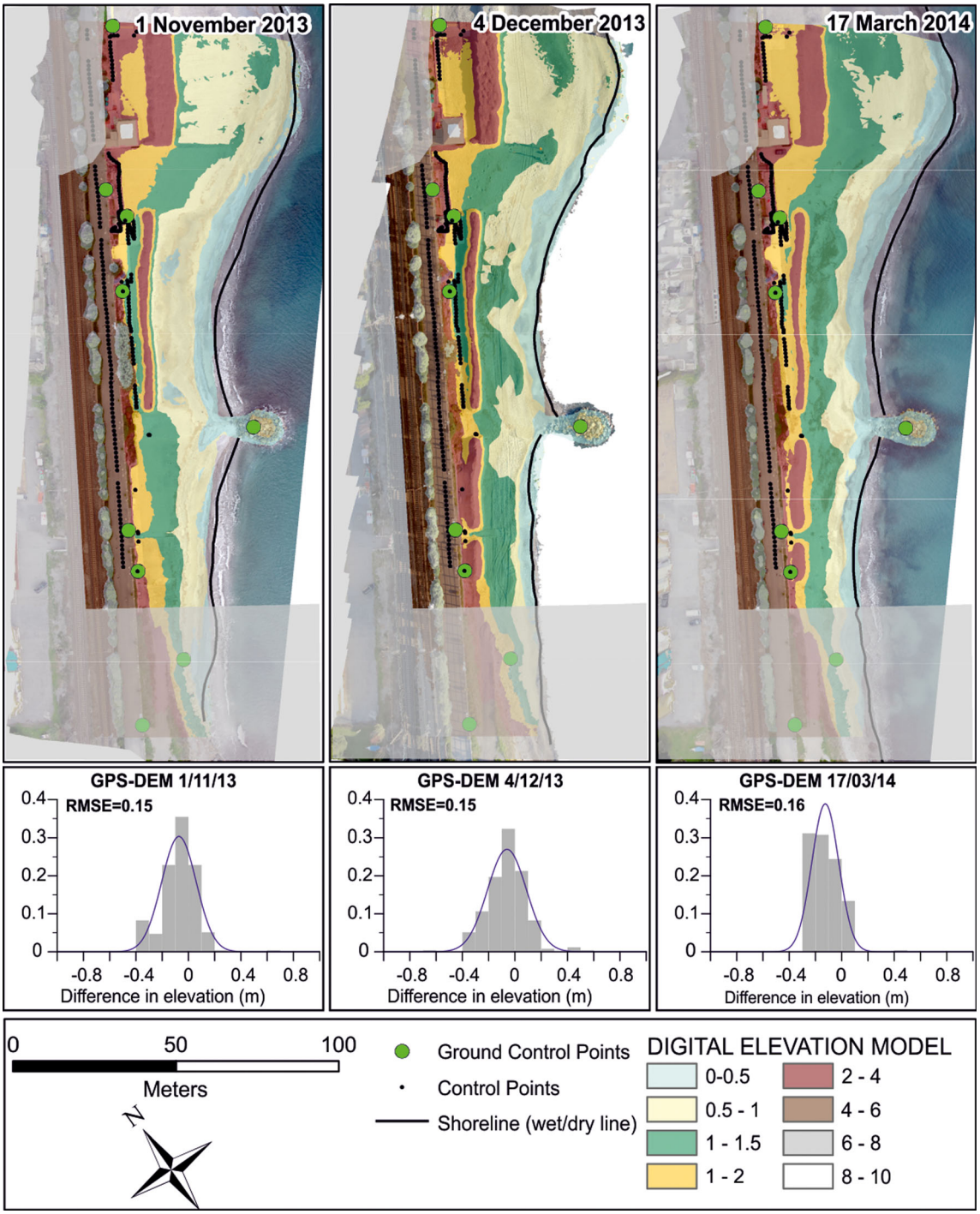

Fig. 2 Orthophotos and digital elevation models obtained from RPAS flights and Photoscan workflow in the three surveys (1 November 2013, 4 December 2013, 17 March 2014). *Three graphs below maps* Frequency distribution of the difference in elevation between the GPS control points shown in the corresponding plots and the elevation extracted from the DEMs. *Grey areas* Zones where less than 4 pictures overlap in at least one of the surveys, making the final DEM less accurate

A further assessment of DEM accuracy is based on the number of photos overlapping at each survey. Figure 2 shows that there were areas where less than four images overlap. In these areas (marked with transparent grey overlay in Fig. 2), the DEM was considered not reliable in the multi-temporal analysis.

The average point cloud density derived from the three RPAS surveys is ~112.7 points/m^2. The total number of points for the whole survey area (also including grey areas in Fig. 2) is 2,208,104. The cell size of the final DEM is 0.095×0.095 m/pixel. Figure 3 shows some of the details of the aerial surveys of this study.

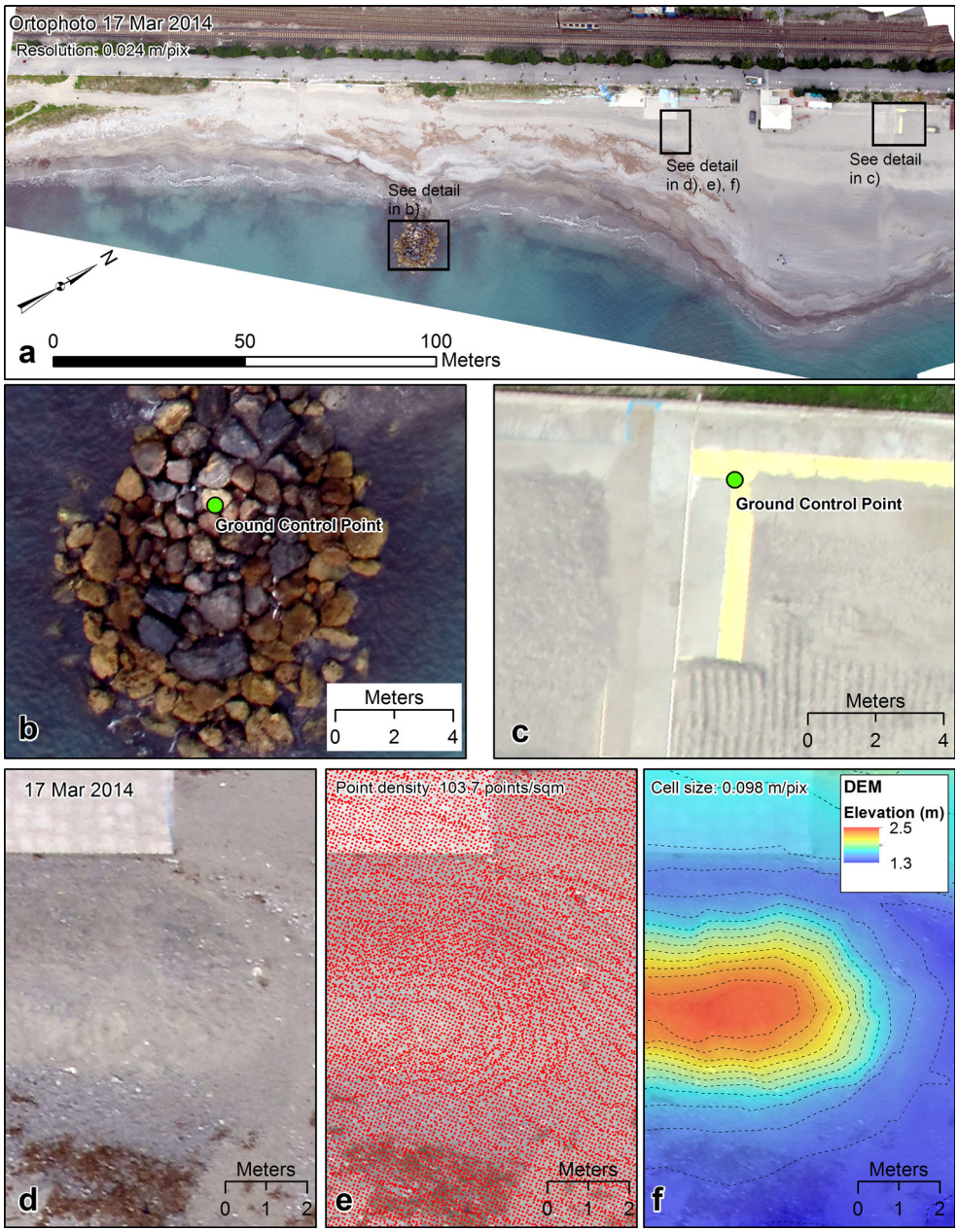

Fig. 3 **a** Orthophoto obtained from RPAS and Photoscan workflow for the survey of 17 March 2014. **b**, **c** Details of locations where two ground control points have been measured. **d**–**f** Respectively, photo, dense cloud point, DEM with contours of one portion of the results obtained for this survey

Sea conditions

From the offshore wave data obtained from the Capo Mele buoy, all storm events which had a significant wave height of >2 m at the buoy (grey lines in Fig. 4) were extracted and used as input to the MIKE 21 spectral wave model. The model was run for each storm and wave data were extracted from the output of each run at about 500 m offshore of the study area (black lines in Fig. 4). The implementation of the model then propagates the wave conditions at the buoy to the beach of interest in the study area.

In the period between the first two surveys (1 November–4 December), the wave buoy registered two storms (10–11 November and 21–22 November 2013; Fig. 4, upper part) which hit the study area mainly at E–NNE angles and with low wave intensity (significant wave height <0.5 m for the first storm, and about 1–1.5 m for the second). In the period between the second and third survey (4 December–17 March 2014), the study area was affected by four storms (25–27 December 2013, 5–6 January 2014, 17–18 January 2014 and 6–10 February 2014) from a prevailing SE direction (Fig. 4, lower part), all of them associated with peak wave heights of 1.5–2 m.

Table 1 Workflow and parameters used in Agisoft Photoscan

Align photo	
Accuracy	High
Pair pre-selection	Disabled
Key point limit	40000
Build mesh (preliminary step to insert GCPs)	
Surface type	Height field
Face count	Medium (30000)
Source data	Sparse cloud
Interpolation	Enabled
Point classes	All
Locate and place GCPs in scene, import GCPs coordinates	
Measurement accuracy (for GCPs)	
Camera accuracy (m)	10
Marker accuracy (m)	0.05
Scale bar accuracy (m)	0.001
Projection accuracy (pix)	0.1
Tie point accuracy (pix)	4
Build dense cloud	
Quality	High
Depth filtering	Aggressive
Build mesh	
Surface type	Height field
Face count	Medium (136012)
Source data	Dense cloud
Interpolation	Enabled
Point classes	All
Generate orthophoto	
Generate DEM	

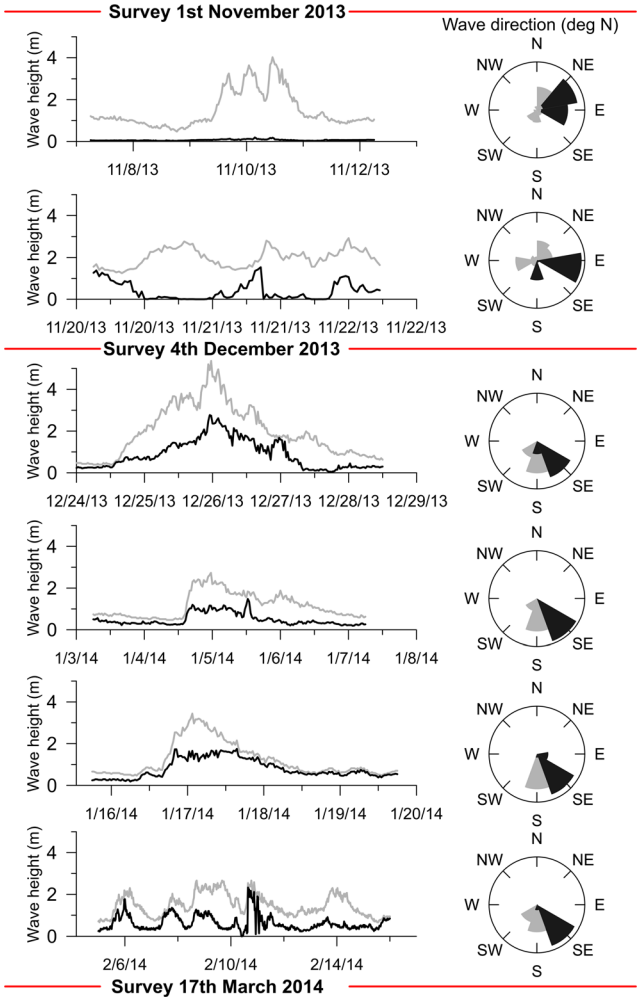

Fig. 4 Wave height and direction for sea storms in the study area as recorded by the Capo Mele buoy (grey line and grey areas in rose diagram; see Fig. 1a for buoy location), and wave height 500 m offshore the study area calculated using the MIKE21 spectral wave module (black line and black areas in rose diagram). Dates in MM/DD/YY format

Coastal changes

The difference between the DEMs obtained on 1 November and 4 December 2013 (Fig. 5a) reveals erosion in the north-eastern part of the study area (transect T1) and deposition towards the central groyne (transect T2). At the southernmost tip of the study area, the volume changes reflect that sediment was artificially removed from the beach and stored in a landward reservoir (transect T3). About 178 m^3 of material was moved by an automatic excavator. The track marks of the excavator can be seen on the orthophoto of 4 December 2013 (Fig. 2).

Another significant volume change involves net erosion in the central part of the beach (marked with number 1 in Fig. 5). Analysis of the orthophotos shows that the "missing" material was associated with a grove of reeds which was cut by the municipal authorities as part of general maintenance works between 1 November and 4 December 2013. Although this aspect is not directly relevant in terms of sediment budgets, it does highlight another possible use of drones and photogrammetry in multi-temporal studies—the gain/loss of vegetation due to natural causes and/or human activities.

Between 1 November and 4 December 2013 the wet–dry line retreated, causing a lowering of the beach profile in the northernmost part and aggradation of the beach in the central part of the study area (Fig. 5a, transects T1–T4). This provides evidence that the E–NNE storms impacting the area between the first two surveys (Fig. 4, upper part) caused significant topographic beach changes, including a shoreline retreat reaching 7 m in some sectors (Fig. 5, transect T3).

A very different evolution can be inferred from the comparison of the DEMs obtained between 4 December 2013 and 17 March 2014 (Fig. 5b). During that time period, strong south-easterly storms caused progradation of the shoreline towards its summer position (compare

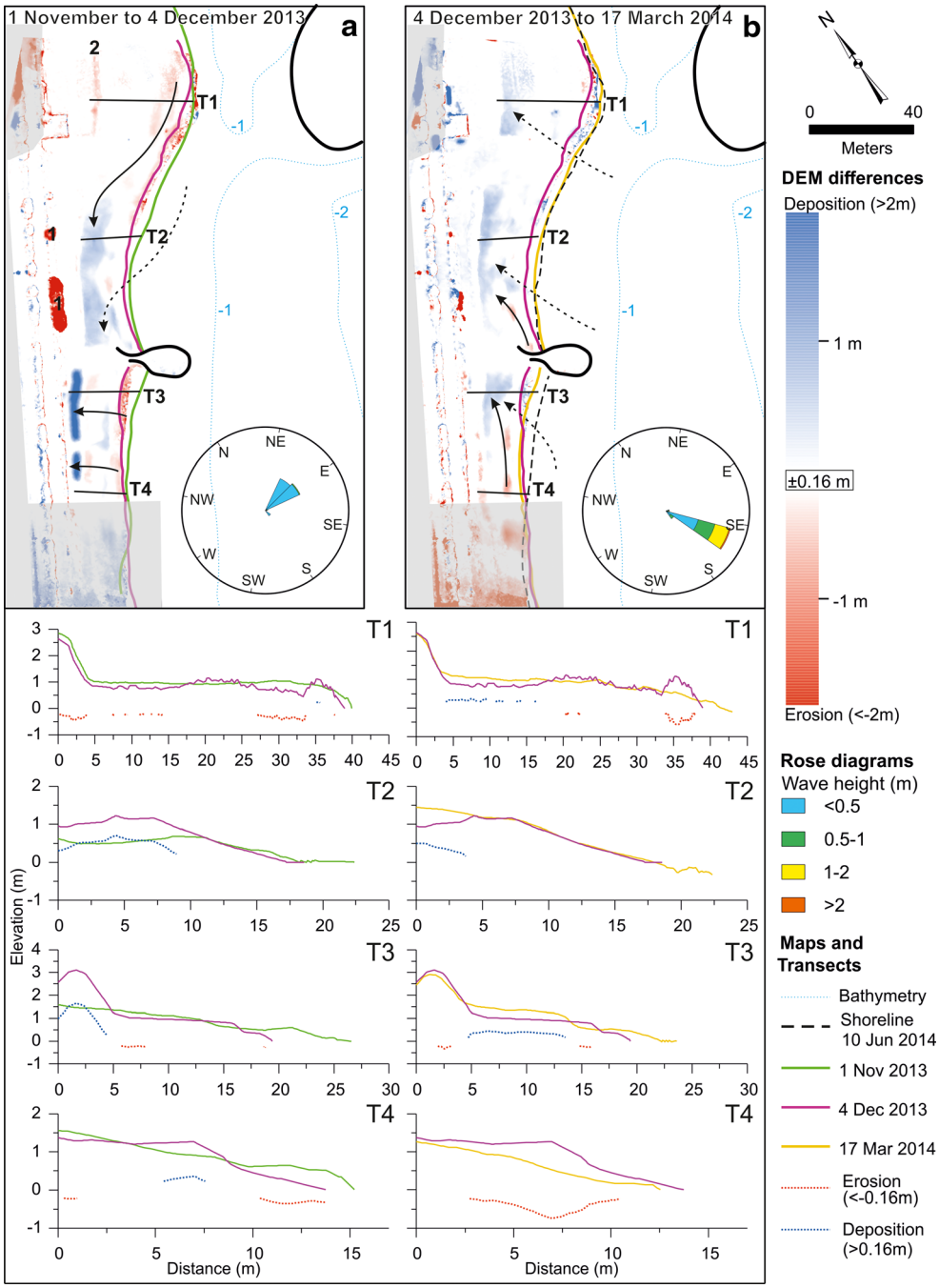

Fig. 5 Difference between digital elevation models obtained from the different surveys (see dates at top). *Solid arrows* Likely movement of sediments onshore, *dashed arrows* likely sediment input from submerged beach. *Light grey areas* Zones where few pictures overlap (see Fig. 2), and therefore where DEM differences have been considered unreliable and are not discussed in the text. *Solid black lines* Coastal defence structures (cf. Figs. 1 and 2). Bathymetric data surveyed in summer 2013 by the Borghetto S.S. Municipality are the same in both frames. *1* Area where a grove of reeds was cut in the time between two surveys, *2* area of 5–10 cm erosion, probably caused by strong NE winds impacting an artificial dune top (visible in Fig. 2). *Bottom panels* Evolution of beach profiles along the four transects outlined in the maps, including changes along these profiles

the shoreline survey of 17 March 2014 with that of June surveyed with DGPS, shown as dashed line in Fig. 5b) and a general aggradation of the beach. This aspect is visible in the T1, T2 and T3 transects of Fig. 5. As only a small area of erosion can be identified at the southernmost tip (where the presence of the rocky promontory of Capo Santo Spirito blocks further sediment inputs; Fig. 1b), it is likely that a large part of the sediment was imported from the shallow submerged area in front of the beach.

Discussion

RPAS as beach monitoring tool

Beach monitoring is subject to tradeoffs between the duration, extent, cost, accuracy and resolution of spatiotemporal surveys. As an example, if one wants to understand the short-term evolution (weeks to months) of a coastal system, traditional in situ measurements can be used with sufficient temporal resolution but they provide only limited areal coverage

Table 2 Comparison between DEM Z accuracies obtained in this and other studies employing UAV and photogrammetric techniques

Reference	RMSD z (m)	Flight height (m)	Comparison method	Photogrammetry technique
This work	0.16	77±0.6	GPS control points	Agisoft Photoscan
Niethammer et al. (2012)	0.31	100–200	Terrestrial laser scanner	VMS (2010), Otto and Chau (1989)
Hugenholtz et al. (2013)	0.29	200	GPS control points	Trimble's Inpho photogrammetric processing software
Grenzdörffer et al. (2008)	0.27	300	GPS control points	Leica Photogrammetry Suite (LPS) 9.1
Udin and Ahmad (2012)	0.63	100	GPS control points	ERDAS Orthobase 8.6
Harwin and Lucieer (2012)	0.04	50	GPS control points	PMVS2 (Harwin and Lucieer 2012)
Mancini et al. (2013)	0.11	40	GPS control points	Agisoft Photoscan

and three-dimensional information (e.g. along transects). On the other hand, airborne orthophotography and lidar provide good spatial resolution but the high cost often prohibits surveys at short time intervals. Similar tradeoffs are common in other research disciplines such as habitat monitoring and wildlife conservation.

The use of small RPAS for remote sensing, landscape mapping and environmental monitoring partially overcomes such problems because they can provide data at high and adjustable frequency (Everaerts 2008; Delacourt et al. 2009; Niethammer et al. 2012; Hugenholtz et al. 2013; Stumpf et al. 2013; Ouédraogo et al. 2014). Typically, small RPAS are of relatively low cost (€ 5,000–10,000), and the small dimensions (few tens of centimetres and usually <5 kg) make them easily and rapidly deployable. In the present study area, RPAS and photogrammetry yielded three sets of orthorectified photographs and DEMs spanning a period of 5 months. In each case, the study area (0.01 km^2) was mapped within 8 minutes. This survey efficiency is low if compared with airborne surveys (e.g. lidar) but it is high if compared with laser scanner or DGPS surveys. The final vertical accuracy (±16 cm) of the DEM produced is in line with most studies using similar techniques (Table 2).

It is worth noting that the smoothness and uniformity of sediment surfaces limits the effectiveness of classical matching algorithms (Fonstad and Marcus 2010). Similar problems might be created by water reflections, which should be masked to avoid unwanted errors in the matching process. Software designed to process aerial images by traditional photogrammetry is not well suited for unstructured image acquisition geometries (Rango et al. 2009). Mancini et al. (2013) showed that the use of the latest image matching algorithms in the SfM workflow leads to the production of high-definition DEMs on sandy surfaces. The main difference between SfM and classical photogrammetry is the use of a new generation of image matching algorithms which allow for unstructured image acquisition, a much higher level of automation, as well as a much greater ease of use and cost efficiency. Indeed, Fonstad and Marcus (2010) demonstrate that SfM can deliver data quality and resolutions which are comparable with lidar and classical photogrammetry.

Weather conditions can be a limiting factor in this methodology, as it is impossible to fly a low-cost drone (such as the Mikrokopter okto XL employed in this study) during rain and with winds or wind gusts of >40 km/h. Light conditions may also affect the expected result of the survey. Depending on the aim of the survey, sunny days should be avoided because areas covered by shadow are not resolved appropriately by the algorithms.

RPAS and coastal zone management

The results obtained in this study show that RPAS can be effectively used to obtain data to support coastal management. It is possible to detect changes due to human activity involving the movement of sediment on the beach and the removal of vegetation. This facilitates the task of the regional authorities who require detailed environmental evaluations in cases exceeding the threshold of 10 m^3 sediment per linear meter being removed from, added to, or simply moved on a beach. Along the Liguria coastline (as well as other Italian coastal sectors), the artificial movement of sediment usually takes place in autumn (late October). Therefore, one flight at the end of summer (September) and another in early winter (November) should capture all such sediment movements along the coast. Once DEMs and orthophotos are extracted, volumes of sediment removed from or imported to a beach can easily be calculated using common GIS tools. In this study the raster calculator in ArcMap was used, but other solutions are available such as r.mapcalc in GRASS and QGIS, or directly from the cloud points with the free software CloudCompare.

Another management implication of the multi-temporal survey approach presented here is the application of drones to obtain data on the short-term evolution of beach topography after emplacement of infrastructures (according to regional law 1793/2005). Looking only at the yearly evolution of the shoreline in the present study area (Fig. 1c), it might be concluded that the shoreline has advanced after the emplacement of coastal defences, and that it now oscillates around an average position. The data reveal that, when the shoreline retreats after smaller storms from the

east (Fig. 5a), there is a volume gain on the emerged beach and virtually no loss of sediment towards the submerged beach. When a series of strong storms from the southeast hits the shoreline, the data indicate that the beach responds with aggradation and progradation, suggesting a net transport of sediment from the submerged beach to the emerged one (Fig. 5b). It is also worth noting that three average-intensity south-easterly storms are sufficient to restore the shoreline to its summer position.

Conclusions

The management of sandy coasts relies on beach monitoring to gather data on the intensity and rates of beach evolution, their monitoring being subject to tradeoffs between accuracy, costs and resolution of the surveys. The last 4 years have seen an exponential increase of research activities based on data collection by drones, whereby the following points should be highlighted.

- Flying platforms have become smaller and capable of lifting more weight, and sensors are increasingly being tailored specifically for drone applications.
- The learning curve for drone pilots is becoming less steep and is counterbalanced by national regulations putting limits to the flying areas, among other things also requiring specific pilot training and risk assessments of the flight operations.
- In coastal environments, the application of SfM and MVS methods to drone-derived photographs may prove challenging due to the uniform nature of the landscape. Nevertheless, the applicability of new-generation SfM methodology in defining the geometry of rocky coasts has been demonstrated by Ružić et al. (2014) and, for sandy coasts, by Mancini et al. (2013).
- Flights in coastal areas might be difficult due to the risks of gusty winds or rapid changes in meteorological conditions, corrosion due to marine spray requiring frequent maintenance of the drone.

Despite the limitations highlighted above, this study shows that remotely piloted aircraft systems coupled with structure from motion and multi-view stereo techniques can be successfully employed to investigate beach topographic changes. Along the coastline of the Municipality of Borghetto Santo Spirito (Italy, northwestern Mediterranean), surveying a given coastal sector three times in 5 months revealed that:

- The digital elevation models are accurate within ±16 cm. The resolution achieved for orthophotos is 0.024 m/pixel, and for DEMs it is 0.095 m/pixel.
- Differences between digital elevation models obtained at different times can be analyzed by means of common GIS tools to gather insights on topographic beach changes.
- Lower-intensity E–NNE storms caused general erosion resulting in a lowering of the beach profile and shoreline retreat which, in some sectors, amounted to 7 m. By contrast, higher-intensity storms from the SE caused a general advancement of the shoreline (~5 m) associated with deposition of sediments (aggradation) in some parts of the beach.
- It is possible to detect human-induced beach changes due to, for example, moving of sediments. Governmental regulations can be enforced using drones.

Acknowledgements This work is part of the project MIRAMAR funded by the PO CRO European Social Fund, Regione Liguria 2007-2013 Asse IV 'Capitale Umano / Human Capital'. A. Rovere acknowledges funding by the Institutional Strategy of the University of Bremen via the German Excellence Initiative and ZMT, the Leibniz Center for Tropical Marine Ecology. We wish to acknowledge C. Cavallo and Regione Liguria for providing baseline data and local datasets. We thank Matteo Vacchi (CEREGE, CNRS) and Luigi Mucerino (University of Genoa) for useful discussions. We are grateful to colleagues of the MEDFLOOD INQUA 1203 project for discussion and input. We acknowledge Geom. A. Billeci and the staff of the Municipality of Borghetto S.S. for collaboration. Part of the datasets shown in Fig. 1 have been derived from Regione Liguria cartographic data (www.ambienteinliguria.it, INSPIRE-compliant metadata links: Metadata1, Metadata2, Metadata3, Metadata4). We acknowledge useful assessments and corrections from two anonymous reviewers as well as the journal editors B.W. Flemming and M.T. Delafontaine, which improved the original manuscript.

Compliance with ethical standards

Conflict of interest The authors declare that there is no conflict of interest with third parties.

References

Alexander PS, Holman RA (2004) Quantification of nearshore morphology based on video imaging. Mar Geol 208(1):101–111

Anderson K, Gaston KJ (2013) Lightweight unmanned aerial vehicles will revolutionize spatial ecology. Front Ecol Environ 11:138–146. doi:10.1890/120150

Berni JAJ, Zarco-Tejada PJ, Suárez L, Fereres E (2009) Thermal and narrowband multispectral remote sensing for vegetation monitoring from an unmanned aerial vehicle. IEEE Trans Geosci Remote Sens 47:722–738

Bird E (1987) The modern prevalence of beach erosion. Mar Pollut Bull 18:151–157

Blodget HW, Taylor PT, Roark JH (1991) Shoreline changes along the Rosetta-Nile Promontory: monitoring with satellite observations. Mar Geol 99:67–77

Brignone M, Schiaffino CF, Isla FI, Ferrari M (2012) A system for beach video-monitoring: beachkeeper plus. Comput Geosci 49:53–61

Casella E, Rovere A, Pedroncini A, Mucerino L, Casella M, Cusati LA, Vacchi M, Ferrari M, Firpo M (2014) Study of wave runup using numerical models and low-altitude aerial photogrammetry: a tool for coastal management. Estuar Coast Shelf Sci 149:160–167. doi:10.1016/j.ecss.2014.08.012

Colomina I, Molina P (2014) Unmanned aerial systems for photogrammetry and remote sensing: a review. ISPRS J Photogramm Remote Sens 92:79–97

Corsini S, Inghilesi R, Franco L, Piscopia R (2006) Italian Waves Atlas. Agenzia per la Protezione dell'Ambiente e per i Servizi Tecnici (APAT) and University of Rome, 3

Delacourt C, Allemand P, Jaud M, Grandjean P, Deschamps A, Ammann J, Cuq V, Suanez S (2009) DRELIO: an unmanned helicopter for imaging coastal areas. J Coastal Res SI 56:1489–1493

DHI (2012) Mike21 spectral wave module. Scientific documentation, Danish Hydraulic Institute (DHI)

Eltner A, Baumgart P, Maas H-G, Faust D (2015) Multi-temporal UAV data for automatic measurement of rill and interrill erosion on loess soil. Earth Surf Process Landf 40(6):741–755. doi:10.1002/esp.3673

Everaerts J (2008) The use of unmanned aerial vehicles (UAVs) for remote sensing and mapping. Int Arch Photogramm Remote Sens Spat Inf Sci 37:1187–1192

Ferrari M, Cabella R, Berriolo G, Montefalcone M (2014) Gravel sediment bypass between contiguous littoral cells in the NW Mediterranean Sea. J Coastal Res 30:183–191

Fierro G, Berriolo G, Ferrari M (2010) Le spiagge della Liguria occidentale – analisi evolutiva. Regione Liguria – Ass. Pianificazione territoriale, Urbanistica Ed

Fiori E, Comellas A, Molini L, Rebora N, Siccardi F, Gochis DJ, Tanelli S, Parodi A (2014) Analysis and hindcast simulations of an extreme rainfall event in the Mediterranean area: the Genoa 2011 case. Atmos Res 138:13–29

Floreano D, Wood RJ (2015) Science, technology and the future of small autonomous drones. Nature 521(7553):460–466

Fonstad MA, Marcus WA (2010) High resolution, basin extent observations and implications for understanding river form and process. Earth Surf Process Landf 35(6):680–698

Grenzdörffer GJ, Engel A, Teichert B (2008) The photogrammetric potential of low-cost UAVs in forestry and agriculture. Int Arch Photogramm Remote Sens Spat Inf Sci 31(B3):1207–1214

Hapke C, Richmond B (2000) Monitoring beach morphology changes using small-format aerial photography and digital softcopy photogrammetry. Environ Geosci 7:32–37

Harley MD, Turner IL, Short AD, Ranasinghe R (2010) Assessment and integration of conventional, RTK-GPS and image-derived beach survey methods for daily to decadal coastal monitoring. Coastal Eng 58:194–205

Hartley R, Zisserman A (2003) Multiple view geometry in computer vision. Cambridge University Press, Cambridge

Harwin S, Lucieer A (2012) Assessing the accuracy of georeferenced point clouds produced via multi-view stereopsis from unmanned aerial vehicle (UAV) imagery. Remote Sens 4(6):1573–1599

Holthuijsen LH, Booij N, Herbers T (1989) A prediction model for stationary, short-crested waves in shallow water with ambient currents. Coast Eng 13:23–54

Hugenholtz CH, Whitehead K, Brown OW, Barchyn TE, Moorman BJ, LeClair A, Riddell K, Hamilton T (2013) Geomorphological mapping with a small unmanned aircraft system (sUAS): feature detection and accuracy assessment of a photogrammetrically-derived digital terrain model. Geomorphology 194:16–24

James MR, Robson S (2012) Straightforward reconstruction of 3D surfaces and topography with a camera: accuracy and geoscience application. J Geophys Res Earth Surf 117, F03017. doi:10.1029/2011JF002289

Kroon A, Davidson MA, Aarninkhof SGJ, Archetti R, Armaroli C, Gonzalez M, Medri S, Osorio A, Aagaard T, Holman RA, Spanhoff R (2007) Application of remote sensing video systems to coastline management problems. Coast Eng 54(6):493–505

Lee JM, Park JY, Choi JY (2013) Evaluation of sub-aerial topographic surveying techniques using total station and RTK-GPS for applications in macrotidal sand beach environment. J Coast Res SI 65:535–540

Littmann T (2000) An empirical classification of weather types in the Mediterranean basin and their interrelation with rainfall. Theor Appl Climatol 66:161–171

Mancini F, Dubbini M, Gattelli M, Stecchi F, Fabbri S, Gabbianelli G (2013) Using unmanned aerial vehicles (UAV) for high-resolution reconstruction of topography: the structure from motion approach on coastal environments. Remote Sens 5(12):6880–6898. doi:10.3390/rs5126880

McGranahan G, Balk D, Anderson B (2007) The rising tide: assessing the risks of climate change and human settlements in low elevation coastal zones. Environ Urban 19:17–37

Morton RA, Leach MP, Paine JG, Cardoza MA (1993) Monitoring beach changes using GPS surveying techniques. J Coast Res 9(3):702–720

Niethammer U, James MR, Rothmund S, Travelletti J, Joswig M (2012) UAV-based remote sensing of the Super Sauze landslide: evaluation and results. Eng Geol 128:2–11

Orlandi A, Pasi F, Onorato LF, Gallino S (2008) An observational and numerical case study of a flash sea storm over the Gulf of Genoa. Adv Sci Res 2:107–112

Otto GP, Chau TKW (1989) Region-growing algorithm for matching of terrain images. Image Vision Comput 7(2):83–94

Ouédraogo MM, Degré A, Debouche C, Lisein J (2014) The evaluation of unmanned aerial system-based photogrammetry and terrestrial laser scanning to generate DEMs of agricultural watersheds. Geomorphology 214:339–355

Parodi A, Boni G, Ferraris L, Siccardi F, Pagliara P, Trovatore E, Foufoula-Georgiou E, Kranzlmueller D (2012) The "perfect storm": from across the Atlantic to the hills of Genoa. EOS Trans Am Geophys Union 93(24):225–226

Pasi F, Orlandi A, Onorato LF, Gallino S (2011) A study of the 1 and 2 January 2010 sea-storm in the Ligurian Sea. Adv Sci Res 6:109–115

Pérez-Alberti A, Trenhaile AS (2015) An initial evaluation of drone-based monitoring of boulder beaches in Galicia, north-western Spain. Earth Surf Process Landf 40(1):105–111

Rango A, Laliberte A, Herrick JE, Winters C, Havstad K, Steele C, Browning D (2009) Unmanned aerial vehicle-based remote sensing for rangeland assessment, monitoring, and management. J Appl Remote Sens 3(1):033542–033542

Rebora N, Molini L, Casella E, Comellas A, Fiori E, Pignone F, Siccardi F, Silvestro F, Tanelli S, Parodi A (2013) Extreme rainfall in the Mediterranean: what can we learn from observations? J Hydrometeorol 14:906–922

Rovere A, Casella E, Vacchi M, Parravicini V, Firpo M, Ferrari M, Morri C, Bianchi CN (2014) Coastal and marine geomorphology between Albenga and Savona (NW Mediterranean Sea, Italy). J Maps 11(2):1–9

Ružić I, Marović I, Benac Č, Ilić S (2014) Coastal cliff geometry derived from structure-from-motion photogrammetry at Stara Baška, Krk Island, Croatia. Geo-Mar Lett 34(6):555–565

Sartini L, Mentaschi L, Besio G (2014) How an optimized meteocean modelling chain provided 30 years of wave hindcast statistics: the case of the Ligurian Sea. In: Proc XXXIV Int Conf Coastal Engineering, Seoul, South Korea, 15–20 June

Saye SE, Van der Wal D, Pye K, Blott SJ (2005) Beach–dune morphological relationships and erosion/accretion: an investigation at five sites in England and Wales using LIDAR data. Geomorphology 72(1):128–155

Scharstein D, Szeliski R (2002) A taxonomy and evaluation of dense two-frame stereo correspondence algorithms. Int J Comput Vision 47:7–42

Seitz S, Curless B, Diebel J, Scharstein D, Szeliski R (2006) A comparison and evaluation of multi-view stereo reconstruction algorithms. In: Proc CVPR '06 I.E. Computer Society Conf Computer Vision and Pattern Recognition, vol 1. IEEE Computer Society, Washington, DC, pp 519–526

Small C, Nicholls RJ (2003) A global analysis of human settlement in coastal zones. J Coast Res 19:584–599

Stockdon HF, Sallenger AH, List JH, Holman RA (2002) Estimation of shoreline position and change using airborne topographic lidar data. J Coast Res 18:502–513

Stumpf A, Malet JP, Kerle N, Niethammer U, Rothmund S (2013) Image-based mapping of surface fissures for the investigation of landslide dynamics. Geomorphology 186:12–27

Szeliski R (2010) Computer vision: algorithms and applications. Springer, Heidelberg

Taborda R, Silva A (2012) COSMOS: a lightweight coastal video monitoring system. Comput Geosci 49:248–255

Theuerkauf EJ, Rodriguez AB (2012) Impacts of transect location and variations in along-beach morphology on measuring volume change. J Coast Res 28(3):707–718

Trigo IF, Bigg GR, Davies TD (2002) Climatology of cyclogenesis mechanisms in the Mediterranean. Mon Weather Rev 130:549–569

Turki I, Medina R, Coco G, Gonzalez M (2013) An equilibrium model to predict shoreline rotation of pocket beaches. Mar Geol 346:220–232

Udin WS, Ahmad A (2012) The potential use of rotor wing unmanned aerial vehicle for large scale stream mapping. Int J Sci Eng Res 3(12)

Ullman S (1979) The interpretation of structure from motion. Proc R Soc Lond B Biol Sci 203(1153):405–426

Vacchi M, Montefalcone M, Bianchi CN, Morri C, Ferrari M (2010) The influence of coastal dynamics on the upper limit of the *Posidonia oceanica* meadow. Mar Ecol 31(4):546–554

Vacchi M, Rovere A, Schiaffino CF (2012) Monitoring the effectiveness of re-establishing beaches artificially: methodological and practical insights into the use of video transects and SCUBA-operated coring devices. Int J Soc Underw Technol 30:201–206

Vacchi M, Montefalcone M, Schiaffino CF, Parravicini V, Bianchi CN, Morri C, Ferrari M (2014) Towards a predictive model to assess the natural position of the *Posidonia oceanica* seagrass meadows upper limit. Mar Pollut Bull 83(2):458–466

Verhoeven G (2011) Taking computer vision aloft—archaeological three-dimensional reconstructions from aerial photographs with PhotoScan. Archaeol Prospect 18:67–73

VMS (2010) Official VMS Software Homepage. http://www.geomsoft.com (accessed 1 August 2010)

Watts AC, Ambrosia VG, Hinkley EA (2012) Unmanned aircraft systems in remote sensing and scientific research: classification and considerations of use. Remote Sens 4:1671–1692

Westoby MJ, Brasington J, Glasser NF, Hambrey MJ, Reynolds JM (2012) 'Structure-from-Motion' photogrammetry: a low-cost, effective tool for geoscience applications. Geomorphology 179:300–314

Woodget AS, Carbonneau PE, Visser F, Maddock IP (2015) Quantifying submerged fluvial topography using hyperspatial resolution UAS imagery and structure from motion photogrammetry. Earth Surf Process Landf 40(1):47–64

Wulder MA, Hall RJ, Coops NC, Franklin SE (2004) High spatial resolution remotely sensed data for ecosystem characterization. Bioscience 54(6):511–521

Young A, Ashford S (2006) Application of airborne Lidar for seacliff volumetric change and beach-sediment budget contributions. J Coast Res 22:307–318